J Mater Sci (2006) 41:6362–6373
DOI 10.1007/s10853-006-0712-5

Transformation of Poly(dimethylsiloxane) into thin surface films of SiO_x by UV/Ozone treatment. Part I: Factors affecting modification

F. D. Egitto · L. J. Matienzo

Received: 30 January 2004 / Accepted: 13 July 2005 / Published online: 22 August 2006

Abstract UV/ozone treatment of poly(dimethylsiloxane) (PDMS) was used to produce thin surface films of SiO_x. Films of PDMS were applied by spin-coating onto gold-coated silicon wafers having (100) orientation. Characterization of the UV/ozone system was performed to map the spatial distribution of intensities of UV radiation. This mapping was used to ensure reproducible modification of films and to aid in the understanding of modification as measured by advancing contact angle using deionized water and x-ray photoelectron spectroscopy (XPS). Rutherford backscattering spectroscopy (RBS) was used to measure thickness of the PDMS films. Treatment reduced the wetting angle, in some cases from a value greater than 100° to a value less than 5°. High resolution XPS spectra were used to study the nature of the modified PDMS film and its relationship to the characteristics of the unmodified PDMS. High resolution XPS spectra in the Si 2*p* region show that O–Si–C bonds in the siloxane, observed prior to treatment, are converted to SiO_x, where x is between 1.6 and 2. Modified films also contain some oxidized carbon components. The time required to reduce the contact angle to a minimum value was greater for the thicker PDMS film samples. The effects of ozone alone (without UV) and UV radiation at 184.9 and 253.7 nm (without ozone) were also investigated. The results of UV/ozone treatment are compared to results achieved by means of plasma surface oxidation.

F. D. Egitto (✉) · L. J. Matienzo
Endicott Interconnect Technologies, Inc., 1701 North Street, Endicott, NY 13760, USA
e-mail: egittofd@eitny.com

Introduction

Polydimethylsiloxane (PDMS) is a transparent, commercially-important polymer based on an inorganic backbone. PDMS is well-suited to plastic molding processes [1]. It is biocompatible and, as such, is a good material for use in surgical procedures such as implants for plastic surgery, as components for catheters, to encase electrode and pacemaker leads, and in prostheses [2]. It is commonly used in the fabrication of micro-electro-mechanical-systems (MEMS), for example, microfluidic devices used for flow injection analysis [3, 4]. PDMS ''stamps'' with patterned relief on the surface are used for the manufacture of nanostructures with dimensions as small as 30 nm, a technique known as soft lithography [5].

The surface of organo-silicon films (like PDMS) can be transformed to a silicon-oxide by a variety of techniques. Seyferth [6] reported the pyrolytic degradation of high molecular weight PDMS to silicon oxide films. One technique that can be employed for modification of polymers and, more specifically, transformation of organo-silicon films into silicon oxides, is low-temperature plasma oxidation [7, 8]. Plasmas used for this application are ionized gases at reduced pressures. Energy is supplied to free electrons by an applied electric field. These energetic electrons ionize and excite atoms and molecules, and dissociate molecules in the gas. Although electron energies in the plasma are quite high, i.e., high enough to induce ionization of atoms or molecules with which they collide, the gas temperature is quite low, near room temperature. Polymer modification is most commonly achieved using oxygen plasmas. Decomposition of organic materials is initiated by reaction with atomic oxygen from the

plasma followed by desorption of volatile by-products. Conversion of organo-silicon materials to silicon oxides is a phenomenon that is well documented for exposure to oxygen plasma environments [7, 9–12]. In particular, polysiloxanes have been known as negative e-beam resists since the early 1970s [9]. Processing of materials can be performed ''in the plasma'' or ''remote from the plasma.'' In the former configuration, substrates reside directly in the chamber housing the plasma. The plasma exists at a greater electrical potential than any surface with which it is in contact, and positive ions from the plasma are accelerated in a direction normal to these surfaces. These ions can attain energies from several electron volts (eV) to greater that 1.0 keV and, by virtue of their kinetic energy, can enhance the rates of chemical reactions at polymer surfaces and/or physically remove (sputter) material from the surface. In the ''remote'' configurations, samples reside in a location outside the influence of electrical potentials and electric fields and, therefore, these samples are not subjected to energetic ion bombardment.

Since there are no volatile silicon-oxides, oxygen plasmas are not effective in removing silicon. During etching of silicon-containing polymers, it is believed that silicon-containing fragments diffuse to the polymer surface where they are converted to SiO_2. The inorganic SiO_2 film functions as an increasingly effective etching barrier (Fig. 1) [7, 12]. Hence, oxygen plasma etching results in an initial thickness loss and a gradual slowing of polymer erosion until etching ceases. Owen and Smith [11] observed oxidation of PDMS to occur in nitrogen, argon and helium plasmas, as well. They suggested residual air or water vapor in the plasma chamber, or oxygen in the polymer itself, as potential sources of oxygen.

Organic removal can also be accomplished by exposure to laser radiation, particularly at wavelengths in the ultraviolet (UV) region where many polymers absorb quite well. Absorption is followed by polymer decomposition [13]. Graubner et al. [14] investigated the ablation behavior of PDMS using 266 nm laser radiation. It was observed that high fluence (energy per unit area per laser pulse) levels were required to induce ablation, i.e., PDMS does not absorb well at 266 nm. However, UV radiation at shorter wavelengths has been used to convert organo-silicon materials to silicon oxides [15, 16]. Exposure of thick films of silsesquioxanes to high fluence excimer laser radiation (193 nm) was shown to produce thick silicon dioxide films for commercial abrasion-resistant coatings [15]. Similar results were obtained using low pressure mercury (184.9 nm) and zinc (213.9 nm) lamps. In addition, UV lamps have been used to transform silicides to SiO_2 [17].

Plasma and laser techniques utilize equipment that can require an appreciable capital investment. An alternative approach that utilizes reactive oxygen and UV radiation is UV/ozone treatment. The apparatus for this technique is quite modest, usually consisting of a UV source, e.g., a low-pressure mercury vapor lamp, and a chamber to house the UV source and the sample(s). Processing is almost always performed in air at atmospheric pressure. In comparison with plasma and laser systems, UV/ozone equipment is relatively inexpensive. An overview addressing UV/ozone cleaning technology and its applications has been given by Vig [18].

A low pressure mercury vapor lamp with a quartz envelope emits strongly at two wavelengths, 184.9 and 253.7 nm. Oxygen molecules absorb strongly at 184.9 nm and dissociate to form atomic oxygen [19] that reacts with O_2 to form ozone

$$h\upsilon(184.9\text{nm}) + O_2(^3\Sigma_g^-) \rightarrow O_2*(^3\Sigma_u^-) \rightarrow O(^3P) + O(^3P)$$

$$h\upsilon(184.9\text{nm}) + O_2(^3\Sigma_g^-) \rightarrow O_2*(^3\Sigma_u^-) \rightarrow O(^1D) + O(^3P)$$

$$O + O_2 + M \rightarrow O_3$$

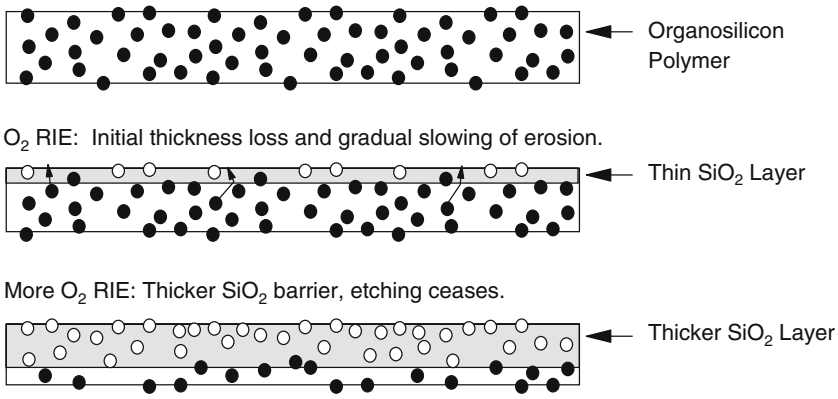

Fig. 1 Simplified schematic representation illustrating conversion using oxygen plasma of an organo-silicon layer to a ''glassy'' surface with progressive reduction, and eventual cessation, of polymer etching. Closed circles represent Si in an organo-silicon environment. Open circles represent Si in a silicon dioxide environment

where M is a third body such as O, O_2, O_3, or N_2 [20–22]. Ozone absorbs at 253.7 nm:

$$O_3 + h\upsilon(253.7nm) \rightarrow O_2 + O$$

Both atomic oxygen and ozone can react strongly with organic materials [19]. Absorption of UV radiation by polymers and organic compounds, can lead to formation of free radicals, formation of excited molecules, or, if the organic material's ionization potential is low enough, formation of ions. Ultimately, the organic radicals react with atomic oxygen or ozone to form low molecular weight, volatile fragments, like CO_2 and H_2O, that can desorb from the surface. As such, UV/ozone processing has been used effectively to remove thin layers of organic contaminants. However, its effectiveness in this regard is somewhat limited to organic materials. In particular, removal of organosilicon compounds does not occur. For PDMS, UV/ozone treatment is effective in removing the organic portion of the PDMS while the siloxane component is converted to silicon oxides [23]. This mechanism is similar to that postulated by Taylor and Wolf [12] for O_2 plasma ''anodization'' of Si-containing polymers whereby the formation of small Si fragments diffuse to the polymer surface where they are converted to an SiO_2 etching mask. Mirley and Koberstein [24] reported that Langmuir-Blogett films prepared from diacid-terminated poly(dimethylsiloxane) can be transformed to ultrathin SiO_x films by exposure to UV/ozone at room temperature and atmospheric pressure. Furthermore, Niwano et al. [25, 26] have reported oxidation of monocrystalline silicon in UV/ozone ambients. Using photoemission and infrared absorption measurements, they reported formation of a 0.5 nm SiO_2 film. It was suggested that this oxide film functions as a protective layer for adsorption of adventitious carbon impurities onto the Si substrate upon exposure to air.

For a given UV/ozone system configuration, relatively few parameters can be varied to affect the rate of etching and modification. The two parameters most readily investigated are position in the chamber and duration of the cleaning process. Spatial nonuniformities in etching and modification rates are related to variation in UV intensity and variation in ozone concentration. UV intensity variations arise due to lamp configuration and losses due to absorption in air and ozone. Hence, nonuniformities in intensity and ozone concentration are somewhat convoluted.

The present paper presents the results of treatment of PDMS deposited onto gold-coated silicon wafers to produce SiO_x surfaces. Characterization of the UV/ozone system is reported in terms of spatial distribution of light intensity and degree of film modification. Modification in the UV/ozone system is compared with plasma oxidation processes. Characterization of treated and untreated film surfaces was performed using x-ray photoelectron spectroscopy (XPS) and measurement of advancing DI water contact angles. An attempt was made to separate the relative contributions of the individual components (i.e., various wavelengths of UV and reaction with atomic oxygen and ozone) that contribute to film modification. The effect of PDMS film thickness on the rate of modification is also reported.

Experimental

Films were formed on polished silicon wafers having a crystalline orientation of (100) so that smaller rectilinear pieces of reproducible size and shape could be obtained by cleaving along orthogonal planes. Unless otherwise indicated, samples used for experiments were about 10 mm square.

PDMS film preparation

The PDMS film was deposited onto gold-coated silicon wafers having a diameter of 125 mm. Gold films on the silicon wafers had been vapor-deposited to a thickness of 78 nm. The gold barrier between the silicon wafer and the PDMS film allowed differentiation between the silicon in the PDMS and the silicon in the wafer during chemical analyses. Thin PDMS coatings were invisible to the unaided eye. Since both the thin PDMS films and the gold scratch easily, marks visible in the gold layer indicated areas of the invisible PDMS coatings that may have been damaged by handling so that these areas could be avoided during analyses. The gold surface also served as a reference layer for determining the thickness of PDMS films. The effects of UV/ozone treatment on the PDMS films were found to be far more reproducible when the gold was cleaned of adventitious organic contaminants for 10 min in the UV/ozone chamber prior to coating with PDMS.

Films of PDMS were spin-coated from solution onto the gold-coated silicon wafers using a Headway Research Inc. Model EC101D-R485 photo-resist spinner. The spin speed was 4000 rpm for 30 seconds. PDMS solutions were prepared by diluting Huls Petrarch Systems polydimethylsiloxane, silanol terminated (catalog #PS341), with Burdick and Jackson high purity grade tetrahydrofuran (THF) solvent. Thickness

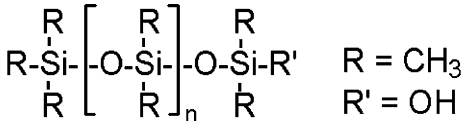

Fig. 2 Chemical structures of PDMS polymers used in this investigation

of the PDMS coating was controlled by varying the concentration of the PDMS in THF. Concentrations in THF included 0.05%, 0.1%, 0.2%, 0.4%, 0.6% and 2.0% (vol/vol). After spinning, films were dried by allowing the solvent to evaporate in air. The chemical structure for PDMS is shown in Fig. 2.

Optical absorption characteristics of the PDMS were determined using a UV–visible spectrum obtained on a Perkin Elmer lambda 9 spectrophotometer. Samples were prepared by sandwiching a large drop of undiluted PDMS between two quartz plates and allowing it to spread to form a film approximately 50 μm thick.

UV/ozone system

UV/ozone treatments were performed in a Uvocs, Inc., model T0606B UV/ozone cleaning system shown schematically in Fig. 3. The UV source is a low-pressure mercury vapor grid lamp, made in a serpentine pattern, with a quartz envelope. The serpentine lamp covers a square area, 152.4 mm on each side. Unless noted, samples were placed 5.7 mm from the lamp envelope. Power density of the lamp was measured using a Spectroline® DRC-100X digital radiometer (® Spectroline is a registered trademark of Spectronics Corporation, Westbury, NY.). Sample temperature was measured using an Omega® (®Omega Engineering, Inc., Stamford, CT) Engineering, Inc., Model 450-AET digital thermometer with a type E thermocouple input.

The effects of different wavelengths of UV radiation (184.9 nm and 253.7 nm) and ozone were studied separately using the cells shown schematically in Fig. 4. To study the effects of UV in the absence of ozone, the cell was evacuated to a pressure of 1.33 Pa and continuously pumped during treatment (Fig. 4d, e). A quartz window allowed treatment using both wavelengths. In some experiments, a potassium bromide (KBr) crystal filter (short wavelength cutoff at 203 nm) was placed between the quartz window and the sample to block the 184.9 nm radiation. Additional experiments were performed in air (i.e., with ozone) where calcium fluoride (CaF_2) crystal filters were used to pass both wavelengths from the lamp, KBr filters were used to block the 184.9 nm radiation, and an opaque disk was used to block all UV radiation from reaching the sample surface in order to study the effects of ozone without UV irradiation of the sample. Multiple crystals were stacked as shown in Fig. 4a–c such that in all cases, the top surfaces of the crystal filters (including the quartz) and the opaque disk were placed at a distance of 5.7 mm from the lamp to provide equivalent optical path lengths in air for all experiments.

Plasma system

A detailed description of the system used for plasma treatment is given in reference [27]. Samples were placed on the RF electrode (cathode) of the reactive ion etching (RIE) system (chemical etching enhanced by bombardment of ions from the plasma). The cathode, covered with a quartz plate, had a diameter of 292 mm. RF power (at 13.56 MHz) was 300 W, chamber pressure was 46.6 Pa (0.35 Torr) and total gas feed flow rate of oxygen (O_2) was 70 standard cubic centimeters per minute (SCCM). The RIE system is shown schematically in Fig. 5a. For several experiments, to perform modification in the absence of ion bombardment, a second quartz plate was placed above the sample such that the distance between the quartz-covered cathode and the second plate was less than the thickness of the space-charge sheath. That is, no plasma was sustained in the vicinity of the sample and treatment was due solely to reaction of neutral atomic oxygen. This configuration is shown schematically in Fig. 5b.

Contact angle measurements

Advancing DI water contact angles on treated and untreated samples were measured with a Rame-Hart, Inc., model A-100 goniometer with optical protractor, using a sessile drop technique and drop volumes between 1 and 2 mm^3. Measurements were made

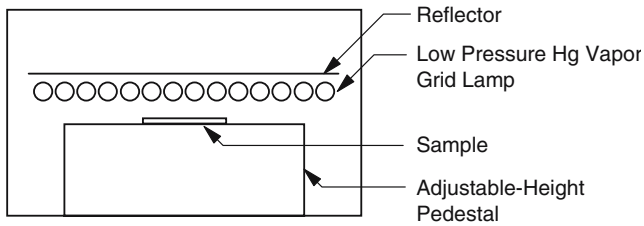

Fig. 3 Schematic illustration of a UV/ozone cleaning system

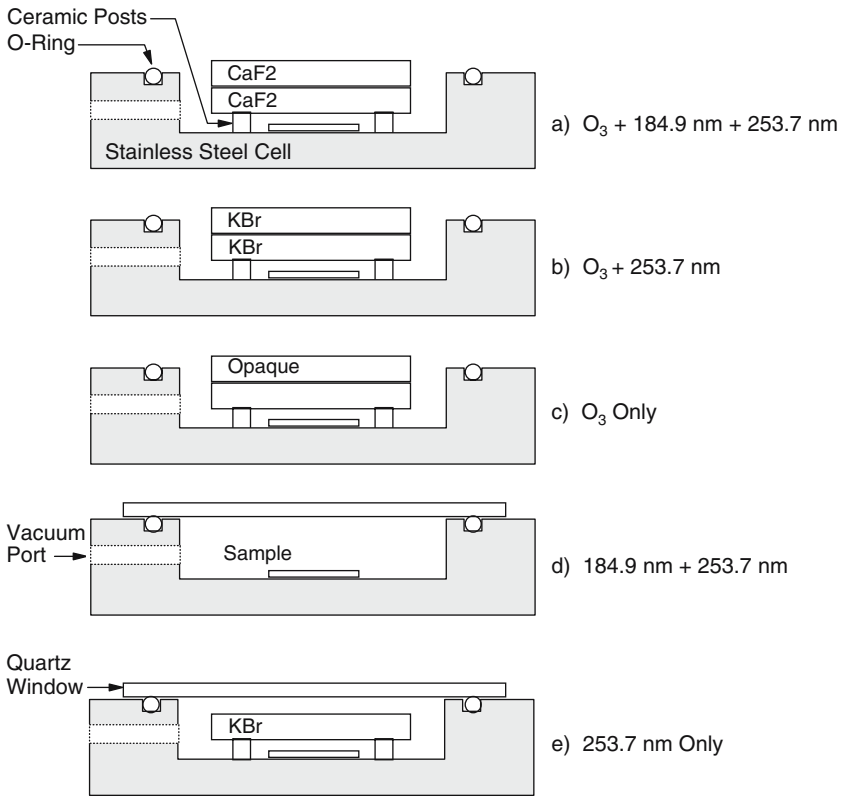

Fig. 4 Configuration of test cells for investigating the effects of the various reactive components of the UV/ozone cleaning system

immediately following treatment. Contact angles were recorded within 30 s from initial application of the drop. Separate samples were used for each data point. Results obtained in this manner were found to be very consistent and reproducible.

X-ray photoelectron spectroscopy (XPS)

XPS was performed in a PHI-5500 Multiprobe spectrometer equipped with a hemispherical analyzer using monochromatized AlK_{α} rays for excitation with a spot size of 800 μm. Survey and high-resolution spectra were collected with pass energies of 158 and 11.8 eV, respectively. Binding energies were referenced to the hydrocarbon peak at 284.8 eV. All spectra were collected at angle of 65° between the surface of the sample and the analyzer of the spectrometer. High-resolution XPS spectra in the C 1*s* and Si 2*p* regions were used to determine the contributions due to different chemical environments, and to follow them as a function of UV/ozone treatment.

Rutherford backscattering spectroscopy (RBS)

The RBS instrument used for measurement of PDMS film thickness consisted of a tandem accelerator to produce a He^{2+} ion beam of 2.1 MeV. The typical geometry of this apparatus has been described elsewhere [28]. The thickness of PDMS films deposited at known concentrations (from 0.4 to 2.0%) in THF was estimated by the relative shift of the underlying gold layer, calculated using spectral simulation described by Doolittle [29]. Density of PDMS was assumed to be 1000 kg/m^3.

Results and discussion

UV/ozone system characterization

Sample surfaces remain relatively cool during exposure, even during extended treatments. Temperature of a sample exposed to UV/ozone treatment at 5.7 mm from the lamp envelope is shown as a function of time in Fig. 6.

Power density for 253.7 nm radiation as a function of lateral position in the chamber is shown for different lamp-to-sample separations in Fig. 7. Each curve was obtained by moving the radiometer in 1.0 cm increments from the rear to the front of the chamber, along a line that dissected the grid lamp. Therefore, the zero point on the x-axis corresponds to a point below the geometric center of the grid lamp. As expected, lamp intensity is greatest at positions nearer to the lamp. In addition, less lateral variation in lamp intensity occurs when measurements are

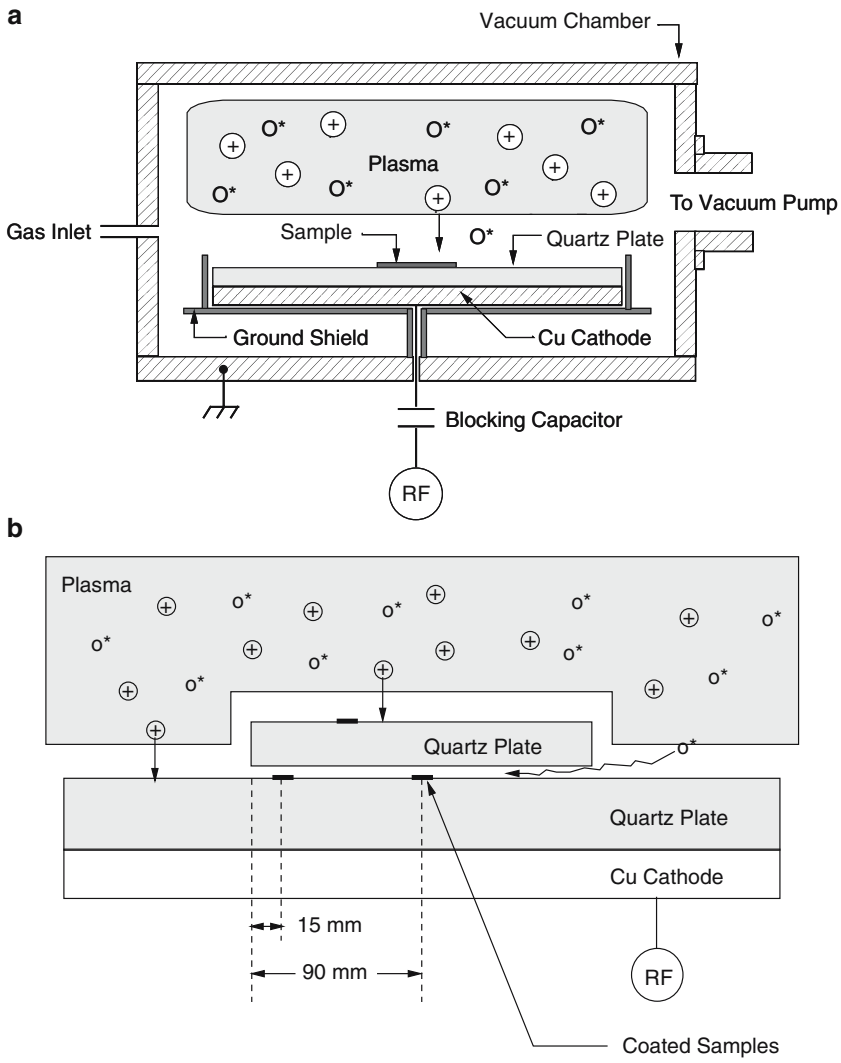

Fig. 5 (**a**) Schematic diagram of RIE system. (**b**) Configuration of RIE system used for treatment of films in the absence of bombardment by energetic ions

taken closer to the lamp. Since ozone absorbs at 253.7 nm, the intensity of the 253.7 nm radiation is a function of the ozone concentration. Since this concentration was not measured, no further attempt is made here to explain the spatial behavior of the lamp intensity.

UV/Ozone treatment of PDMS films

PDMS film thickness, measured using RBS, is shown as a function of the polymer's concentration in THF in Fig. 8. The relationship between concentration and thickness of the films is linear. Thickness at concentrations less than 0.4% was interpolated (including a data point at zero thickness for a concentration of zero percent). The extrapolated value of thickness at 0.1% is near 2.5 nm.

The spatial variation of the rate of reduction in contact angle is related to the intensity of UV radiation. This is shown as a function of lateral position in the chamber and as a function of distance from the lamp in Fig. 9a and b, respectively. Samples were treated for four minutes (Fig. 9a) or five minutes (Fig. 9b). For all other experiments, samples to be treated were placed at positions near the center of the chamber where variation in lamp intensity was minimal.

Figure 10 shows contact angle as a function of UV/ozone treatment time for PDMS-coated samples having two different sizes, namely 10 mm square and 50 mm square. Sample size had little effect on modification. In addition, measurements of contact angles made at a number of different positions on the larger sample were within a range of four degrees for each treatment time, i.e., no sample edge effects were observed.

Atomic compositions obtained from XPS survey spectra are shown for the surfaces of the as-received gold, and for samples of PDMS having various thickness, before and after exposure to UV/ozone treatment, in Table 1. The gold surface exhibits some level

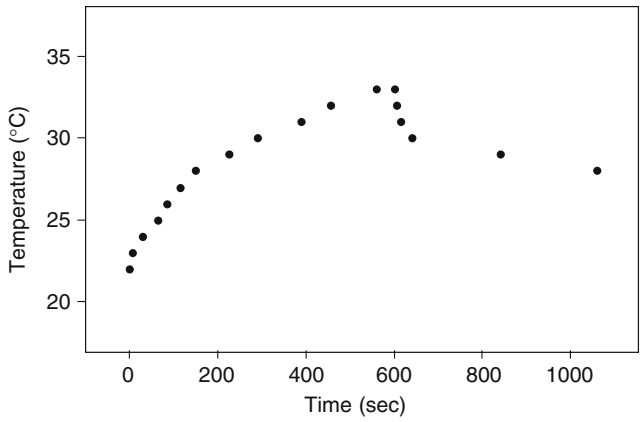

Fig. 6 Temperature of a sample exposed to UV/ozone treatment at a distance of 5.7 mm from the lamp envelope as a function of exposure duration. The lamp was turned off at 600 s

of adventitious carbon and oxygen. In fact, contact angles on UV/ozone-cleaned gold surfaces were observed to increase from 2° to 20° after sitting in air for 10 min following UV/ozone cleaning of the gold. The appearance of a signal corresponding to gold in the spectrum for the 2.5 nm thick PDMS-coated sample is consistent with the sampling depth of XPS performed at normal incidence, typically greater than 5 nm. The concentration of carbon decreases following UV/ozone treatment, however a large increase is observed in the level of oxygen. Silicon is still detected. The signal due to gold does not increase significantly with treatment. Reduction in contact angle from a value greater than 100° to a value less than 5° is due to the presence, on the surface, of SiO_x and oxidized carbon species. In fact, differences in measured values of Si/O and C/O between the thin (2.5 nm) and thick (48 nm) films are likely due to the presence of oxidized carbon at the polymer surface. The contribution for oxidized carbon represents a larger percentage of the overall signal for the thinner film than for the thicker films. In the latter case, the total film thickness (modified surface plus bulk) exceeds the depth of analysis of the XPS.

High resolution XPS spectra in the Si 2*p* region are shown for PDMS samples, 2.5 nm thick, before and after ten minute UV/ozone exposure in Fig. 11. The peak at 102.3 eV, observed prior to treatment, can be attributed to O–Si–C bonds in the siloxane and the peak at 103.4 eV, observed following treatment, corresponds to SiO_x, where x is between 1.6 and 2 [17]. For a thin PDMS film treated for a time sufficient to reduce the contact angle to its minimum value, all of the silicon that remains on the surface is converted to an oxide. Because of the relative concentrations of silicon and oxygen shown in Table 1, it appears that some oxygen must also be associated with carbon residues. UV/ozone treatment does not completely

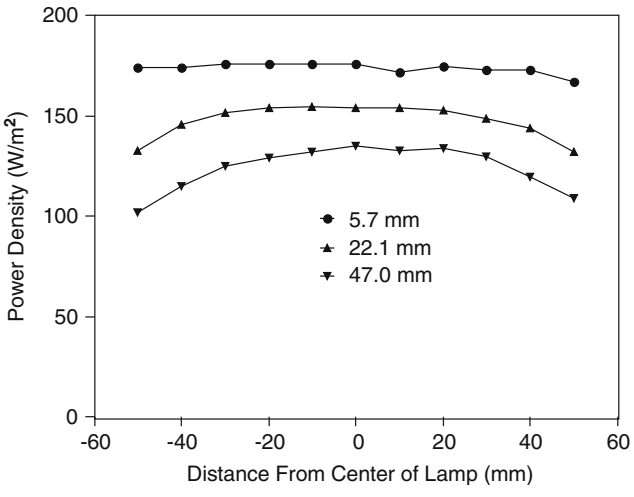

Fig. 7 Power density for 253.7 nm radiation as a function of lateral position in the chamber, measured at various lamp-to-sample separations

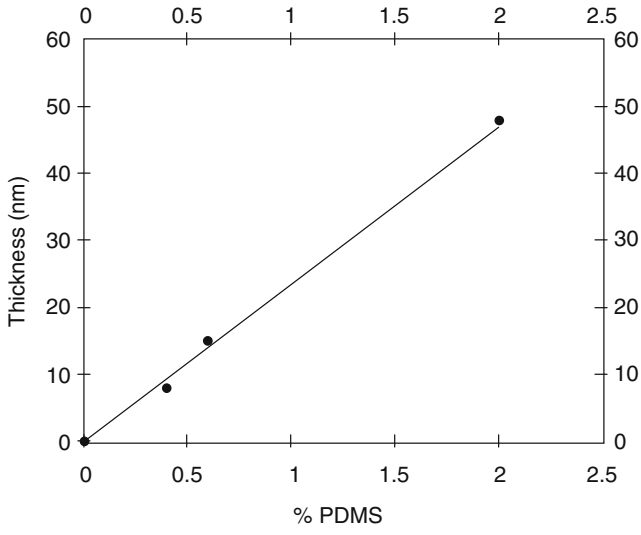

Fig. 8 PDMS film thickness, measured using RBS, as a function of the polymer's concentration in THF

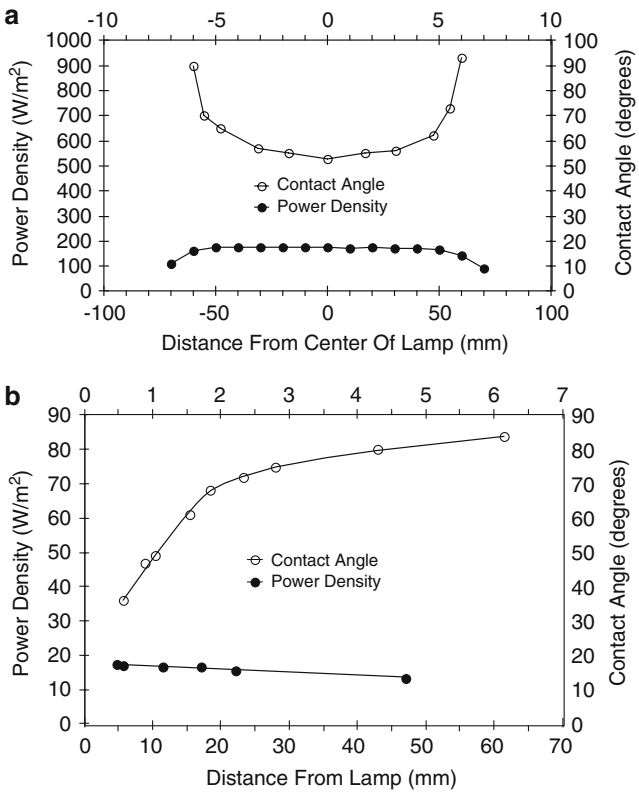

Fig. 9 Spatial variation in advancing DI water contact angle on PDMS-coated samples (**a**) as a function of lateral position in the chamber, measured on samples treated for 4 min at a distance of 5.7 cm from the lamp envelope, and (**b**) as a function of distance from the lamp, measured on samples treated for 5 minutes at the center of the UV/ozone chamber. In each case, the spatial variation in contact angle is compared to the spatial variation in power density for 253.7 nm radiation

remove PDMS fragments, but modifies the film considerably. The rate of PDMS modification, as determined by measurement of contact angle and high resolution XPS spectra in the Si 2*p* region, decreases as the thickness of the PDMS film increases. Reduction in contact angle results from conversion of silicones to silicon-oxides as well as oxidation of carbon-containing groups. Using ellipsometry, Mirley and Koberstein [24] reported a depth of reaction with UV/ozone (30 min exposure) as great as 14.1 nm for Langmuir-Blogett (LB) films prepared on gold from diacid-terminated poly(dimethylsiloxane), a depth of modification comparable to the thickness of PDMS films used in the present investigation. These investigators discussed a mechanism for conversion of silicones to SiO_2 that was dependent upon diffusion of ozone into the silicone.

For the thinnest film of the present investigation (2.5 nm), it is likely that the full thickness of the PDMS is converted to silicon oxides. This is supported by Fig. 11, which shows the apparent complete conversion of the signal from O–Si–C character to SiO_x character for a film whose thickness is less than the sampling depth of the XPS. The presence of carbon and excessive amounts of oxygen detected by XPS indicates that the film contains, in addition to SiO_x, other carbon-containing species. Although diffusion of ozone (or atomic oxygen) into the PDMS may play a role in determining the depth of modification in UV/ozone environments [24], it is possible that during the initial stages of treatment, there is sufficient replenishment of siloxane to the surface, similar to the mechanism discussed in connection with Fig. 1, for which it was proposed that silicon-containing fragments diffuse to the polymer surface where they are converted to SiO_2 by the UV/ozone treatment. In any case, for thicker films of PDMS subjected to longer treatment times, the SiO_x film becomes thicker, and the ratio of Si to O within the sampling depth of the XPS becomes that of SiO_2. Using rf and microwave plasma modification techniques, Hillborg et al. [30] reported conversion of PDMS to an SiO_x film surface having a thickness of 130–160 nm, much thicker than the thickest PDMS films used in the present investigation. It was proposed that an increase in contact angle observed after treat-

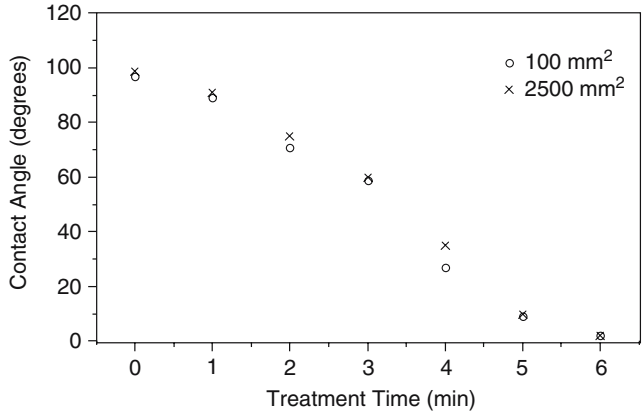

Fig. 10 Advancing DI water contact angle as a function of UV/ozone treatment time for PDMS-coated samples having two different sizes, namely 10 mm square and 50 mm square

Table 1 Atomic compositions obtained from XPS survey spectra for surfaces of as-received gold, and for samples of PDMS having various thickness, before and after exposure to UV/ozone treatment. Data for treatments in MW plasma, corona discharge, and UV at 172 nm are shown for comparison

	Atomic percent			
	C	O	Au	Si
As-received Au	25.9	13.1	61	0
PDMS (theoretical)	50	25	–	25
2.5 nm PDMS, untreated	48.5	28.6	10.2	12.7
2.5 nm PDMS, 10 min UV/ozone	25.7	51.8	12	10.5
5.0 nm PDMS, untreated	41	29	6	24
5.0 nm PDMS, 10 min UV/ozone	17	55	4	24
48 nm PDMS, Untreated	50	25.5	–	24.5
48 nm PDMS, 13 min UV/ozone	22.5	54	–	23.5
PDMS, 3 min oxygen MW Plasma [30]	32.9	42.4	–	24.7
PDMS-based elastomer, 18 min corona discharge [36]	29.4	44.9	–	25.7
PDMS, 40 min UV (172 nm) [32]	4	63	–	33

ment was potentially due to diffusion of low molar mass PDMS species to the surface. Of course, it is not expected that there be a discrete boundary between the SiO_x and the bulk PDMS film. Efimenko et al. [31] reported that UV/ozone treatment of Sylgard-184 PDMS resulted in a dense material whose top 5 nm reached a composition of about 50% SiO_2, with a diminishing concentration of SiO_2 at greater depths, a profile that they attributed to the diffusivity of oxygen in PDMS. In contrast, for treatment with UV only, although conversion to SiO_2 occurred, a dense surface region was not observed, with the top surface attaining a composition having only about 20% SiO_2. This behavior was attributed to recombination of photo-induced radicals in the absence of oxygen.

To aid in understanding the contributions of the various reactive components in the system described in this paper, samples of PDMS film were treated using various configurations (Fig. 4) that allowed exposure to (a) UV (184.9 nm and 253.7 nm) and ozone, (b) UV (253.7 nm only) and ozone, (c) ozone alone, (d) UV alone (184.9 and 253.7 nm) and (e) UV alone (253.7 nm only). In this series of experiments, the sample resided at a distance of 22.7 mm from the lamp to accommodate placement of the various filters. Results of contact angle measurements as a function of treatment time in each of the five configurations is shown in Fig. 12.

In configuration (a), the CaF_2 filter allows exposure of the sample to UV radiation at both 184.9 nm and 253.7 nm, as well as any ozone generated below the filter and reactive species that diffuse around the filter to the PDMS surface. In this case, rate of modification was the greatest. Configuration (b) differs from configuration (a) only with respect to replacement of the CaF_2 filter by a KBr filter. As a result of imposition of the KBr filter, exposure of the samples to radiation at 184.9 nm is eliminated. In addition, no ozone is generated in the region immediately above the surface of the samples so that interaction with ozone is entirely

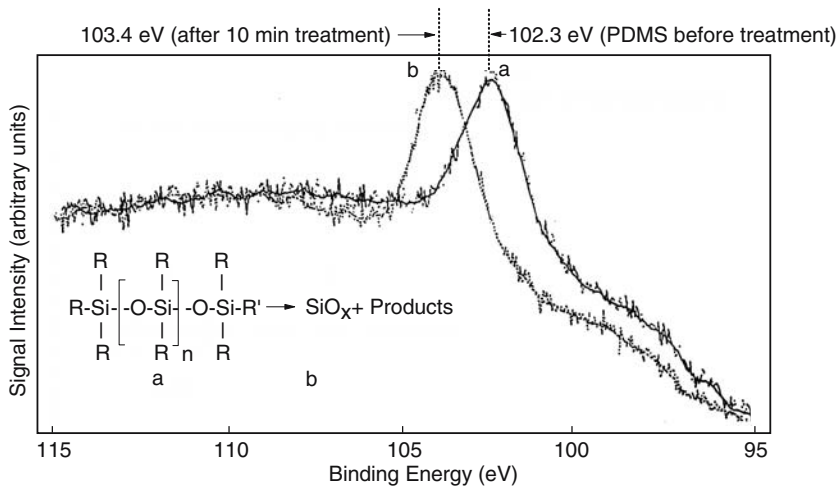

Fig. 11 High resolution XPS spectra in the Si 2*p* region for PDMS samples (2.5 nm thick) before and after ten minute UV/ozone exposure. Signals are shown without background correction

dependent upon diffusion under the filter. Although modification still occurs without the 184.9 nm radiation, the rate of PDMS modification is greatly reduced.

In configuration (c), an opaque material blocked all UV radiation from the sample such that modification occurred only as a result of reactive species that migrated to the surface of the PDMS. Although the presence of ozone (and oxygen atoms) is sufficient for modification of PDMS, change in contact angles is extremely slow (Fig. 12, curve **c**). Only for treatment times on the order of 10^3 minutes (not shown in the graph) was a significant reduction in contact angle observed. Treatment with UV alone, no ozone, resulted in a more rapid reduction in contact angle than was observed for ozone alone (configuration (d)), but was much slower than the change observed with both UV and ozone, in agreement with Efimenko et al. [31]. Schnyder et al. [32] reported conversion of PDMS films (between 50 and 240 nm thick) to a SiO_2-type structure upon exposure to UV irradiation at 172 nm. Thickness of the resulting SiO_2 film was estimated to be 5–10 nm. Photolysis of PDMS most likely proceeds via side-chain scission producing hydrogen or methyl radicals [33]. These radicals, in turn, may react with PDMS to abstract hydrogen. Polymer radicals resulting either from the photolysis or abstraction reactions may combine to form crosslinks [31, 33] or, in the presence of oxygen, form hydroperoxides which break down to form silanol structures [33]. The resulting polymer surfaces possess higher surface energies than exhibited by the unmodified PDMS. When eliminating irradiation at 184.9 nm (that is, irradiation at 253.7 nm only, in vacuum), configuration (e), no change was observed for PDMS. This is not surprising since PDMS, a saturated polymer, exhibits strong absorption at wavelengths below about 193 nm, but exhibits little or no absorption at 253.7 nm [14].

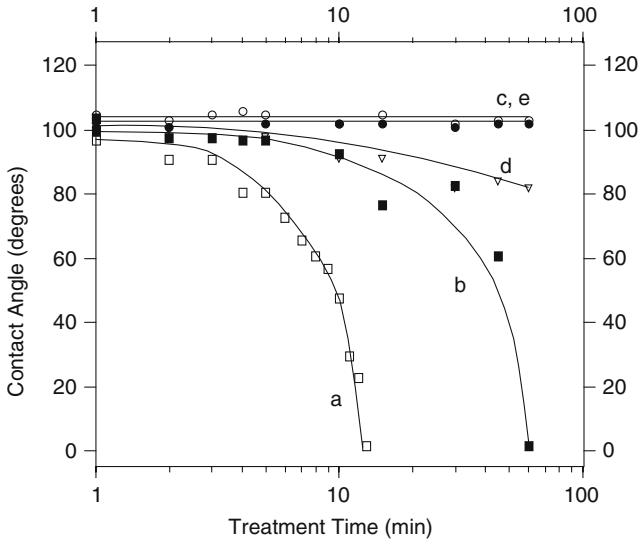

Fig. 12 Advancing DI water contact angle for 2.5 nm PDMS films treated using the cell configurations shown in Fig. 4, measured as a function of UV/ozone treatment time. Curves are labeled **a**-**e** to correlate with the configuration designations given in Fig. 4

Although roughness of treated and untreated PDMS films was not measured in this study, previous studies on polyimide [34] and chitosan [35] polymer films using atomic force microscopy showed no change in surface roughness with UV/ozone treatment. Roughness values (R_a) for the polyimide films were, in all cases, less than 0.5 nm [34]. Hillborg et al. [30] reported smooth films (less than 10 nm) upon plasma treatment of PDMS films. In addition, in the present study, no attempt was made to measure the final thickness of the treated films.

Comparison of UV/ozone and plasma treatments.

Figure 13 shows advancing DI water contact angles as a function of treatment time for samples of 48 nm thick PDMS treated at various locations in the plasma system shown schematically in Fig. 5b. It is apparent that the contact angle decreases with treatment time such that films located nearer to the plasma (edge of the cover plate) are modified more quickly that those located at a more remote location (center of the cover plate). This is due to recombination of reactive oxygen atoms as they diffuse under the cover plate.

Hillborg et al. [30] treated vinyldimethyl-terminated PDMS films (200 nm) downstream from oxygen microwave plasmas (sample remote from the plasma). The configuration of Fig. 5b mimics this configuration since sample under the cover plate are not exposed to bombardment by energetic ions. Hillborg and co-workers [30] demonstrated conversion of the PDMS to an SiO_x-rich layer. For 180 s exposure to the MW plasma, PDMS films changed to a composition that was 42.4% oxygen, 32.9% carbon, and 24.7% silicon. In addition, it was concluded that the thickness of the oxidized layer was on the order of 130 nm, a conversion considerably deeper than observed for the UV/ozone-modified films of the present investigation. In a separate study, Hillborg and Gedde [36] reported a depth of modification on the order of 10–12 nm for corona discharge treatment of an elastomer based on PDMS, similar in depth to the films modified by UV/ozone treatment in the present study.

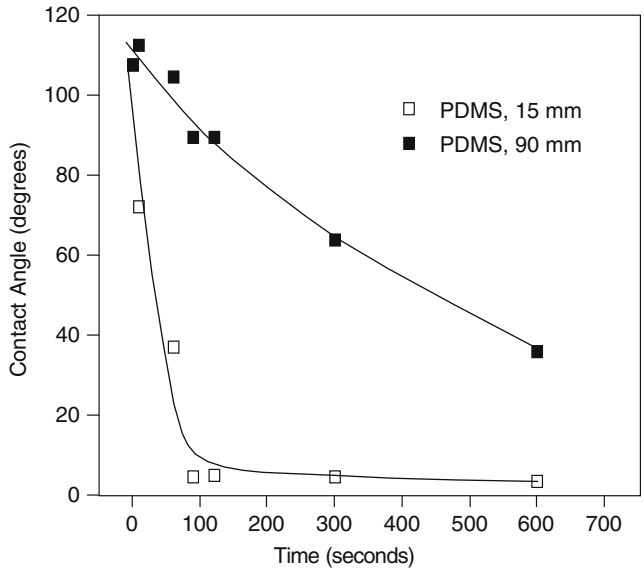

Fig. 13 Advancing DI water contact angle for PDMS films (48 nm thick) treated in a plasma system using the configuration shown in Fig. 5b

Conclusions

The UV/ozone system used in the present investigation has a relatively uniform horizontal distribution of lamp intensity. However the intensity varies considerably with distance from the lamp. The rate of film modification demonstrates a dependence on this intensity. The O–Si–C bonds in the siloxane, observed prior to treatment, are converted to SiO_x, where x is between 1.6 and 2. Some of the oxygen is associated with carbon-containing groups, remnants in the surface SiO_x film. The rate of transformation of the PDMS to a steady state SiO_x-rich surface depends on the PDMS film thickness. PDMS films having thickness of 2.5 nm are transformed through the entire thickness while films having thickness of 48 nm are transformed to a depth on the order of 10 nm. The depth of modification is shallow, and the rate of modification is fastest for the thinner films. For thicker films, it is possible that silicon-containing fragments from the bulk diffuse to the surface until the SiO_2 film is continuous enough and thick enough to inhibit this diffusion, at which point a steady state surface composition is achieved. It is also possible that diffusion of oxygen or ozone into the film may play a rate limiting role. Hence, the thickness of the SiO_2 film formed by UV/ozone modification is somewhat limited. This mechanism is similar to what has been reported for both oxygen plasma and UV/ozone-treated organo-silicon polymers.

Separation of components (chemical and photo) involved in the modification process indicates that neither O_3 alone nor radiation at 253.7 nm alone are effective in modification of the surface. Introduction of the 184.9 nm component of the radiation (to the 253.7 nm component) increases the rate of modification, but not as much as introduction of O_3 to the 253.7 nm component. Of course, the highest rate of modification is achieved when all components (UV, ozone, and atomic oxygen) act simultaneously on the PDMS.

Acknowledgments The authors acknowledge Dr. Steven Fuerniss for assistance with film preparation, and Carlos DeJesus for assistance with film treatment and contact angle measurements.

References

1. Judy JW (2001) Smart Mater Struct 10:1115
2. National Toxicology Program Report Number IMM90006, ''Contact Hypersensitivity Studies in Female B6C3F$_1$ Mice,'' U.S. Department of Health and Human Services
3. Duffy DC, Schueller OJA, Brittain ST, Whitesides GM (1999) J Micromech Microeng 9:211
4. Jo B-H, Lerberghe LM, Motsegood KM, Beebe DG (2000) J Microelectro-mech Syst 9:76
5. Xia Y, Whitesides GM (1998) Angew Chem Int Ed 37:550
6. Seyferth D (1990) Adv Chem Ser, No 224:565
7. Egitto FD, Vukanovic V, Taylor GN (1990) In: D'Agostino R (ed) Plasma deposition, treatment, and etching of polymers, Academic Press, Inc., San Diego, CA, pp 321–422, and references therein
8. Egitto FD, Matienzo LJ (1994) IBM J Res Develop 38(4):423
9. Roberts ED (1973) J Electrochem Soc 120:1716
10. Feneberg P, Krekeler U (1976) US Patent 3, 959, 105
11. Owen MJ, Smith PJ (1994) J Adhes Sci Technol 8(10):1063
12. Taylor GN, Wolf TM, private communication
13. Srinivasan R, Braren B (1990) In: Fouassier J-P, Rabek JF (eds) Lasers in polymer science and technology: applications, vol III. CRC Press, Inc. Boca Raton, Florida, pp 133–179
14. Graubner V-M, Jordan R, Nuyken O, Lippert T, Hauer M, Schnyder B, Wokaun A (2002) Appl Surf Sci 197–198:786

15. Arkles B, Janeiro B, Berry DH, Ezbiansky KA, Composto R In: Proceedings of Silicones in Coatings III, Barcelona, Spain, 28–30 March, 2000, (The Paint Research Association, Teddington Middlesex, UK, 2000) p 1
16. Sharma J, Berry DH, Composto RJ, Dai H-L (1999) J Mater Res 14:990
17. Li J, Mayer JW, Matienzo LJ, Emmi F (1992) Mater Chem Phys 32:390
18. Vig JR (1987) In: Mittal KL (ed) Treatise on clean surface technology. Plenum Press, New York, pp 1–26
19. Rabek JF (1975) In: Bamford CH, Tipper CFH (eds) Comprehensive chemical kinetics: vol 14, Degradation of polymers. Elsevier Scientific Publishing Company, Amsterdam, The Netherlands, pp 423–538
20. Eliasson B, Hirth M, Kogelschatz U (1987) J Phys D: Appl Phys 20:1421
21. Eliasson B, Kogelschatz U (1991) IEEE Trans Plasma Sci 19(6):1063
22. Greenwood OD, Tasker S, Badyal JPS (1994) J Polym Sci A: Polym Chem 32:2479
23. Egitto FD, Matienzo LJ, Spalik JM, Fuerniss SJ (1995) In: Proceedings of the MRS spring meeting:polymer/inorganic interfaces II, 385 MRS, San Francisco, CA, USA, April 17–21, p. 245
24. Mirley CL, Koberstein JT (1995) Langmuir 11:1049
25. Niwano M, Suemitsu M, Ishibashi Y, Takeda Y, Miyamoto N, Honma K (1992) J Vac Sci Technol A 10:3171
26. Niwano M, Kageyama J, Kinashi K, Miyamoto N, Honma K (1992) J Vac Sci Technol A 12(2):465
27. Egitto FD, Emmi F, Horwath RS, Vukanovic V (1985) J Vac Sci Technol B 3:893
28. Green PF, Palmstrom CJ, Mayer JW, Kramer EJ (1985) Macromolecules, 18:501
29. Doolittle LR (1985) Nucl Instrum Methods, B9:344
30. Hillborg H, Ankner JG, Gedde UW, Smith GD, Yasuda HK, Wilkstrom K (2000) Polymer 41:6851
31. Efimenko K, Wallace WE, Genzer J (2002) J Colloid and Interface Sci, 254:306
32. Schnyder B, Lippert T, Kotz R, Wokaun A, Grqubner V-M, Nuyken V-M (2003) Surf Sci 532–535:1067
33. Mckellar JF, Allen NS (1979) Photochemistry of man-made polymers. Applied Science Publishers LTD, London, pp 169–171
34. Sarno D, Egitto FD, Gurumurthy CK, Henderson DW, unpublished results
35. Sarno D, Matienzo LJ, Winnacker SW, unpublished results
36. Hillborg H, Gedde UW (1998) Polymer 39:1991